



UNIVERSITÀ POLITECNICA DELLE MARCHE
Repository ISTITUZIONALE

A functional source separation algorithm to enhance error-related potentials monitoring in noninvasive brain-computer interface

This is a pre print version of the following article:

Original

A functional source separation algorithm to enhance error-related potentials monitoring in noninvasive brain-computer interface / Ferracuti, F.; Casadei, V.; Marcantoni, I.; Iarlori, S.; Burattini, L.; Monteriu, A.; Porcaro, C. - In: COMPUTER METHODS AND PROGRAMS IN BIOMEDICINE. - ISSN 0169-2607. - ELETTRONICO. - 191:(2020). [10.1016/j.cmpb.2020.105419]

Availability:

This version is available at: 11566/275324 since: 2024-07-19T16:14:42Z

Publisher:

Published

DOI:10.1016/j.cmpb.2020.105419

Terms of use:

The terms and conditions for the reuse of this version of the manuscript are specified in the publishing policy. The use of copyrighted works requires the consent of the rights' holder (author or publisher). Works made available under a Creative Commons license or a Publisher's custom-made license can be used according to the terms and conditions contained therein. See editor's website for further information and terms and conditions.

This item was downloaded from IRIS Università Politecnica delle Marche (<https://iris.univpm.it>). When citing, please refer to the published version.

note finali coverage

(Article begins on next page)

Manuscript Details

Manuscript number	CMPB_2019_1520
Title	A functional source separation algorithm to enhance error-related-potentials monitoring in noninvasive brain-computer interface
Article type	Full Length Article

Abstract

Background and Objectives: An error-related potential (ErrP) can be noninvasively and directly measured on the scalp by electroencephalography (EEG), as response, when a person recognizes an error during a task. It has been shown that ErrPs can be automatically detected in tasks with time-discrete feedback, which is widely applied in the field of Brain-Computer Interfaces (BCIs) for error correction or adaptation. In this work, a semi-supervised algorithm, named Functional Source Separation (FSS), was proposed to enhance evoked ErrPs by estimating a spatial filter; the raw EEG signals were then projected into the estimated signal subspace. **Methods:** Data recorded on six subjects were used to evaluate the proposed method against the xDAWN algorithm. FSS and the xDAWN based methods were compared also with the Cz and FCz single channel. In order to evaluate the performance of the proposed approaches, single-trial classification was considered. **Results:** The results, which were presented using the Bayesian linear discriminant analysis classifier, show that FSS (accuracy 0.92, sensitivity 0.95, specificity 0.81, F1-score 0.95) overcomes the other methods (Cz - accuracy 0.72, sensitivity 0.74, specificity 0.63, F1-score 0.74; FCz- accuracy 0.72, sensitivity 0.75, specificity 0.61, F1-score 0.75; and xDAWN accuracy 0.75, sensitivity 0.79, specificity 0.61, F1-score 0.79) in terms of single-trial classification. **Conclusions:** The proposed method increases the single-trial detection accuracy of ErrPs with respect to single channel (Cz, FCz) approach and using xDAWN spatial filter as well.

Keywords	Brain Computer Interface (BCI), Electroencephalography (EEG), Error-related Potential (ErrP), Functional Source Separation (FSS), P300, Spatial filter
Manuscript category	Biomedical signal and image processing methods
Manuscript region of origin	Europe
Corresponding Author	Camillo Porcaro
Corresponding Author's Institution	ISTC-CNR
Order of Authors	Francesco Ferracuti, Valentina Casadei, Ilaria Marcantoni, Sabrina Iarloria, Laura Burattini, Andrea Monteriù, Camillo Porcaro
Suggested reviewers	Ali Mazaheri, Giorgio Arcara, Giovanni Pellegrino, Filippo Zappasodi

Submission Files Included in this PDF

File Name [File Type]

Cover_Letter_CMPB.doc [Cover Letter]

Highlights.docx [Highlights]

CMPB_Ferracuti-Porcaro.docx [Manuscript File]

Conflict of Interest.docx [Conflict of Interest]

To view all the submission files, including those not included in the PDF, click on the manuscript title on your EVISE Homepage, then click 'Download zip file'.

Research Data Related to this Submission

Data set

<http://bnci-horizon-2020.eu/database/data-sets>

R. Chavarriaga, J.D.R. Millán, Learning from EEG error-related potentials in noninvasive brain-computer interfaces, *IEEE Trans. Neural Syst. Rehabil. Eng.* 18 (2010) 381–388. doi:10.1109/TNSRE.2010.2053387.

This dataset corresponds to an experiment on EEG error-related potentials (ErrPs) elicited when the user monitors the behavior of an external device upon which he/she has no control whatsoever. This experiment was one of the first that showed that these correlates could be observed and decoded during monitoring of external agents. Works that make use of this dataset should cite [Chavarriaga and Millán, 2010].

September 23th, 2019

Dear Filippo Molinari,
Editor-in-Chief of Computer Methods and Programs in Biomedicine

enclosed please find a copy of the paper entitled:

A functional source separation algorithm to enhance error-related-potentials monitoring in noninvasive brain-computer interface

by Francesco Ferracuti, Valentina Casadei, Ilaria Marcantoni, Sabrina Iarlori, Laura Burattini, Andrea Monteriù, and Camillo Porcaro, which we intend to submit for a possible publication on *Computer Methods and Programs in Biomedicine*.

First, thanks for managing the review process to improve the quality of the paper and to evaluate it for publication in your Journal.

The present paper proposes a novel spatial filter based on functional source separation (FSS) algorithm for enhancing single-trial classification of error-related potentials in noninvasive brain-computer interface.

The spatial filter obtained by FSS algorithm increases the single-trial detection accuracy (accuracy 0.92, sensitivity 0.95, specificity 0.81, F1-score 0.95) of error-related EEG potentials (ErrPs) with respect to single channel approach (Cz - accuracy 0.72, sensitivity 0.74, specificity 0.63, F1-score 0.74; FCz - accuracy 0.72, sensitivity 0.75, specificity 0.61, F1-score 0.75) and using xDAWN (0.75, sensitivity 0.79, specificity 0.61, F1-score 0.79) spatial filter as well.

Authors report no conflict of interest.

I confirm that there are not any prior conference proceedings or papers related to this work.

No financial support has been received for this study.

I confirm that this work is entirely original and has not been copyrighted, published, submitted, or accepted for publication elsewhere.

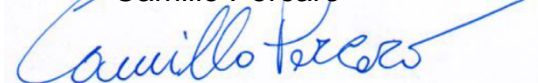
Please address all correspondence concerning this manuscript to me at camillo.porcaro@istc.cnr.it.

Thank you for your consideration of this manuscript.

Looking forward to hearing from you, I remain.

Yours Sincerely

Camillo Porcaro



Highlights

- semi Blind Functional Source Separation (FSS) identify optimal spatial filter for BCI
- FSS algorithm is able to enhance error-related potential (ErrPs) monitoring in non-invasive BCI
- Bayesian linear classification shows higher accuracy for FSS respect to single EEG electrodes
- Bayesian linear classification shows higher accuracy for FSS respect to xDAWN spatial filter

A functional source separation algorithm to enhance error-related-potentials monitoring in noninvasive brain-computer interface

Francesco Ferracuti^a, Valentina Casadei^a, Ilaria Marcantoni^a, Sabrina Iarlori^a, Laura Burattini^a, Andrea Monteriu^a and Camillo Porcaro^{a,b,c,d,e,*}

^a Department of Information Engineering, Università Politecnica delle Marche, Ancona, Italy

^b Institute of Cognitive Sciences and Technologies (ISTC) - National Research Council (CNR), Rome, Italy

^c Research Center for Motor Control and Neuroplasticity, KU Leuven, Leuven, Belgium

^d S. Anna Institute and Research in Advanced Neurorehabilitation (RAN) Crotone, Italy

^e Centre for Human Brain Health, School of Psychology, University of Birmingham, Birmingham, United Kingdom

f.ferracuti@univpm.it; v.casadeibio@gmail.com; i.marcantoni@pm.univpm.it; s.iarlori@univpm.it; l.burattini@univpm.it; a.monteriu@staff.univpm.it; camillo.porcaro@istc.cnr.it

Abstract

Background and Objectives: An error-related potential (ErrP) can be noninvasively and directly measured on the scalp by electroencephalography (EEG), as response, when a person recognizes an error during a task. It has been shown that ErrPs can be automatically detected in tasks with time-discrete feedback, which is widely applied in the field of Brain-Computer Interfaces (BCIs) for error correction or adaptation. In this work, a semi-supervised algorithm, named Functional Source Separation (FSS), was proposed to enhance evoked ErrPs by estimating a spatial filter; the raw EEG signals were then projected into the estimated signal subspace.

Methods: Data recorded on six subjects were used to evaluate the proposed method against the xDAWN algorithm. FSS and the xDAWN based methods were compared also with the Cz and FCz single channel. In order to evaluate the performance of the proposed approaches, single-trial classification was considered.

Results: The results, which were presented using the Bayesian linear discriminant analysis classifier, show that FSS (accuracy 0.92, sensitivity 0.95, specificity 0.81, F1-score 0.95) overcomes the other methods (Cz - accuracy 0.72, sensitivity 0.74, specificity 0.63, F1-score 0.74; FCz- accuracy 0.72, sensitivity 0.75, specificity 0.61, F1-score 0.75; and xDAWN accuracy 0.75, sensitivity 0.79, specificity 0.61, F1-score 0.79) in terms of single-trial classification.

Conclusions: The proposed method increases the single-trial detection accuracy of ErrPs with respect to single channel (Cz, FCz) approach and using xDAWN spatial filter as well.

Keywords: Brain Computer Interface (BCI), Electroencephalography (EEG), Error-related Potential (ErrP), Functional Source Separation (FSS), P300, Spatial filter

*Corresponding author:

Prof. Camillo Porcaro, PhD

Address: Via Palestro 32, 00185 Rome Italy

E-mail address: camillo.porcaro@istc.cnr.it

Phone: +39 06 4436 2370 int 0

AUC: Area Under Curve; BLDA: Bayesian Linear Discriminant Analysis; BCI: Brain-Computer Interface; C: corrected trials; CSP: common spatial filter; EEG: electroencephalography; ErrP: error-related potential; EA: evoked activity; FDR: False Discovery Rate; FSS: Functional Source Separation; ICA: independent component analysis; NC: non-corrected trials; ROC: Receiver Operating Characteristic; SNR: signal-to-noise ratio; SSNR: signal-to-signal plus noise ratio.

1. Introduction

Brain-Computer Interface (BCI) is a noninvasive technology that allows communication between the user's brain and a digital device (e.g. smart wheelchairs, computers, or prosthesis), usually named agent. BCI allows the recognition of the user intention by decoding his neural activity through electroencephalography (EEG) in order to control the agent and improve its performances. Reaching this goal implies high cognitive attention and effort, since the user is asked to continuously pay close attention to the stimuli provided when operating a BCI.

In literature, many works analysed the capability of the BCI to recognize erroneous behaviours of agents directly from the user's brain signals [1–7]. Errors in the recognition of the user's intention elicited potentials called evoked Error-related EEG Potentials (ErrPs). ErrPs were analysed the first time in 1990, in a study about choice-reaction tasks [8]; in the same work the typical wave shape of ErrPs was defined. In this paradigm, the user monitors the agent's actions providing a feedback that can be used to improve the overall performance of the agent. ErrP is physiologically defined as a two-components brain signal, consisting in negative and positive peaks, associated to the response monitoring and error detection processes. Both peaks have originated in the anterior cingulate cortex, a frontal brain structure involved in the cognitive and affective brain processes [9]. Typically, the signal is generated within 500 ms from the erroneous agent decision and the first component is a negative peak at almost 50-100 ms. After the negative peak, a positive peak is generated, further divided into frontocentral and centroparietal components [10].

Works [1,2] are examples where ErrP signals are generated when a user monitors the performance of an agent upon, without performing a direct control. Unlike traditional BCI systems, the user does not provide continuous commands, but only monitors the agent's performance, thus making possible to tailor the agent's behaviour to the user's needs and preferences [3]. Particularly, in the experimental protocol proposed in [1] the user tried to move a cursor towards a target location (either using a keyboard or mental commands). Moreover, that work showed the possibility to recognize and correct erroneous decision of the agent exploiting the user's EEG signals.

The application of ErrPs in BCI technology has increased during the last years, especially for the correction of the system behaviour through what is called reinforcement learning. Precisely, the most common application of ErrP was done in BCI spellers, where during the spelling of a word, a character can be discarded if it is wrong [4]. ErrPs can be involved as a suitable alternative or complementary signal for BCI systems, especially as supervision or feedback signal during the execution of the task [7]. ErrPs have turned out to be used for fixing this problem, as demonstrated in an experiment carried in [5], where a biofeedback based on ErrPs is applied in a closed-loop system for the behavioural correction of a robot. The feasibility to use the ErrPs in combination with brain-machine interface signal to decode the action commands, where the ErrPs solve the erroneous ones, was investigated in [6], whereas, in the context of BCI, authors in [11], investigated whether ErrPs are also elicited when the error is made by the interface during the recognition of the subject's intent. Another research proposed the classification of error-related potentials from EEG during a real-word driving task. While subject was driving, a directional cue was shown before reaching an intersection and the proposed system infers whether the cued direction coincided with the subject's intention [12]. Other works investigated the co-adaptation of human-agent using ErrPs and decoding of ErrPs in tasks with continuous feedback [13,14].

However, the most important challenge of BCI applications relates to the performance, since the control cannot offer a constant level of assistance due to weakness of EEG signals. Consequently, the application of spatial filters to improve the signal-to-noise ratio (SNR) and the single-trial classification is worthy of investigation. Spatial filters are proposed in the literature with the aim to increase the SNR by using a weighted sum of all electrodes rather than relying on a single, or a small sub-set, of EEG channels. Some examples of spatial filters are the so-called xDAWN and the common spatial filter (CSP) [15,16]. Variants and extensions of CSP are proposed in [16–18], trying to overcome the drawbacks of CSP and improve the classification of single-trial EEG. In [19,20], the authors proposed adaptive spatial filters, the former based on ensembles of common spatial pattern patches whereas the latter combines blind source separation and regression analysis.

In this work, Functional Source Separation (FSS) was used to estimate a spatial filter for learning the ErrPs in BCI and it was designed by considering the ErrPs as a functional constraint [21–24]. The final aim was a direct comparison of the FSS [21] with the xDAWN algorithm [15,25] to show the capability of the spatial filters to enhance the evoked ErrPs. Moreover, a single-trial classification was considered to assess the performances of FSS with respect to xDAWN. The FSS- and xDAWN-based methods are also compared with the single channels Cz and FCz, usually selected to monitor ErrPs [1], in terms of single-trial classification.

Section I of this paper presents the experimental protocol, the spatial filters and the classification algorithm used in the study. Section 2 introduces also the idea of using the FSS as spatial filter for learning the ErrPs in BCI. Experimental results are presented in Section 3 including a qualitative evaluation of the spatial filters and the single-trial classification. The conclusions are presented in Section 4.

2. Materials and Methods

In this section the experimental details are presented and the algorithms FSS, xDAWN and Bayesian Linear Discriminant Analysis (BLDA) are described.

2.1 Experimental protocol and dataset description

The considered dataset, whose signals were acquired in the experimental protocols proposed by [1], served as an experiment on EEG ErrPs. Specifically, six subjects (mean age 27.83 ± 2.23 years old) performed two recording sessions (session 1 and session 2) separated by several weeks. Both session 1 and session 2 consisted of 10 blocks: each block corresponded to approximately 50 trials and each trial was about 2000 ms long. In each trial, the user, without sending any command to the agent, only assessed whether an autonomous agent performed properly the task, which consisted in a cursor reaching a target on a computer screen. Specifically, at the beginning of each trial the user was asked to fixate the centre of the screen, and during the trial he/she was asked to monitor the movement of the cursor, knowing the goal of the task. Thus, ErrPs were elicited by monitoring the behaviour of the agent.

Practically, each user was asked to seat in front of a computer screen where a moving cursor, identified by a green square, and a target location, identified by a blue or red square, were displayed. Target could be placed on the left or on the right of the cursor: in the first case it was blue, while in the second case it was red. The working area consisted of 20 locations along the middle horizontal plane of the computer monitor. At each time step (i.e., at each trial) the cursor moved horizontally of discretized steps toward the target location, either the left or right.

Once the target was reached, the cursor remains in place and a new target location was drawn at no more than three positions away from the current cursor position. If the new location fell outside of the working area, it was relocated at the centre of the screen. The probability for the cursor to move in the wrong direction (i.e., opposite to the target location) was set to 0.20. In the paper, the corrected trials (C) refer to trials where the cursor reaches the target, whereas the non-corrected trials (NC) refer to the trials where the cursor moves in the wrong direction and then fails to reach the target.

During the trial, EEG data were recorded at a sampling rate of 512 Hz using a Biosemi ActiveTwo system and placing 64 electrodes according to the standard 10/20 international system.

2.2 EEG pre-processing

The data were re-referenced to common average reference. Off-line bandpass forward-backward filtering between 1 and 10 Hz (Butterworth second order filter) was applied [1]. Since the nature of the experiments may induce lateral eye movements, a semiautomatic independent component analysis (ICA)-based procedure to identify and remove ocular artefacts, cardiac artefacts and environmental noise, without rejecting the contaminated epochs, was applied [26][27].

In this work, the session 1 of each subject was used to train the considered spatial filters and the BLDA classifier while session 2 was used to test the algorithms.

2.3 Functional Source Separation Algorithm

FSS [21,28–34] is a semi-blind source separation method [35] which uses some well-known distinctive features of electrophysiological signals. The aim of FSS is to enhance the separation of relevant signals by exploiting a priori knowledge without renouncing the advantages of using only information contained in original signal waveforms. FSS, analogous to ICA, models the set of EEG recorded signals \mathbf{X} as a linear combination of an equal number of sources \mathbf{s} via a mixing matrix \mathbf{A} . Differing from other constrained ICA models [36–38], FSS identifies a single source at a time, building a contrast function for that source that exploits fingerprint information associated to the neuronal pool to be identified [35]. In general, FSS starts from the original EEG data matrix \mathbf{X} for each source and returns one functional source with the required functional property. This scheme gives us the possibility to extract the functional sources that maximizes the functional behavior in agreement with the functional constraint [35]. A modified cost function (with respect to standard ICA) is defined as: $\mathbf{F} = \mathbf{J} + \lambda \mathbf{R}$ where \mathbf{J} is the statistical constraint normally used in ICA, while \mathbf{R} accounts for the a priori information known about the sources. The relative weight of these two parameters can be adjusted via λ [31]. λ were chosen to both minimize computational time and maximize the functional constraint \mathbf{R} . Moreover, the FSS contrast function \mathbf{F} is optimized by means of simulated annealing [39], thus allowing prior information about the FS to be described by a non-differentiable function.

In the experimental condition proposed in [1], the *a priori* information to be identified is the ERP around 300 ms activated during the target identification. Thus, we identified the functional source underlying the P300 processes maximizing the P300 response named FS_{P300} . The functional constraints used were defined as follows:

$$R_{FS_{P300}} = \frac{1}{(\Delta 1 t_k + \Delta 2 t_k)} \sum_{t_k - \Delta 2 t_k}^{t_k + \Delta 2 t_k} |EA(t)| - \frac{1}{500} \sum_{t=-500}^0 |EA(t)| \quad (1)$$

with the evoked activity (EA), computed by averaging signal epochs of the source FS_{P300} , triggered on the stimulus ($t = 0$); t_k is the time point at which the electric potential power is maximum on the EEG channels around 300 ms post-stimulus; $\Delta 1 t_k$ ($\Delta 2 t_k$) is the time point at which the signal amplitude is 50% of the maximum value before (after) t_k ; the baseline was computed in the time interval from -500 to 0 ms.

2.4 xDAWN

The xDAWN spatial filter allows to enhance the SNR through the unsupervised estimation of the evoked subspace so that the evoked potentials are enhanced by projecting [15,25].

Let $\mathbf{X} \in \mathbb{R}^{N_t \times N_s}$ the matrix of the recorded EEG signals, where N_t is the number of samples and N_s the number of channels, the target stimuli elicited by evoked potential leads to the following model:

$$\mathbf{X} = \mathbf{D}\mathbf{W} + \mathbf{N} \quad (2)$$

where \mathbf{N} is the noise term, \mathbf{D} is the Toeplitz matrix and \mathbf{W} represents the synchronous response with target stimuli. The spatial filter \mathbf{U} is designed in such a way that maximizes the signal-to-signal plus noise ratio (SSNR) of \mathbf{X} . This idea is formulated by the generalized Rayleigh quotient:

$$\hat{\mathbf{U}} = \underset{\mathbf{U}}{\operatorname{argmax}} \frac{\operatorname{trace}(\mathbf{U}^T \hat{\mathbf{W}}^T \mathbf{D}^T \mathbf{D} \hat{\mathbf{W}} \mathbf{U})}{\operatorname{trace}(\mathbf{U}^T \mathbf{X}^T \mathbf{X} \mathbf{U})} \quad (3)$$

where $\hat{\mathbf{W}} = (\mathbf{D}^T \mathbf{D})^{-1} \mathbf{D}^T \mathbf{X}$ and the optimization problem in (3) can be solved by a QR factorization with a singular value decomposition. In order to improve the performance of the xDAWN algorithm, we considered to use a regularization term during the learning stage [40].

The regularization operation allows to overcome the issues related to high-dimensional situations where the applicability of the spatial filter is reduced since it makes direct high dimension matrix operation [40]. To overcome these issues, the empirical, polled covariance matrices considered in the generalized Rayleigh quotient were replaced with:

$$\mathbf{S} = (1 - \gamma)\mathbf{S} + \gamma \cdot \frac{\operatorname{trace}(\mathbf{S})}{d} \mathbf{I} \quad (4)$$

where γ is a hyperparameter to be set and the matrix \mathbf{S} is both $\mathbf{X}^T \mathbf{X}$ and $\hat{\mathbf{W}}^T \mathbf{D}^T \mathbf{D} \hat{\mathbf{W}}$. The experimental results described in the paper refer to the xDAWN algorithm with the addition of the regularization term (γ).

2.5 Bayesian LDA

The detection of the evoked ErrP is performed by the BLDA classifier, which was used in [15] to detect the evoked related potentials spatially filtered by the xDAWN. In this paper, BLDA was adopted also to evaluate FSS based spatial filter and the single-trial classification by using the channels FCz and Cz as well.

Among the proposed classifiers for BCIs, BLDA [41,42] was chosen since it was efficient and fully automatic (i.e., no hyperparameters to adjust).

BLDA aims to fit data \mathbf{x} using a linear function of the form:

$$y(\mathbf{x}, \mathbf{w}) = \sum_{j=1}^M w_j \phi_j(\mathbf{x}) = \mathbf{w}^T \boldsymbol{\phi}(\mathbf{x}) \quad (5)$$

where $\boldsymbol{\phi}(\mathbf{x})$ is the feature vector and assuming that the target variable is equal to $t = y(\mathbf{x}, \mathbf{w}) + \epsilon$, where ϵ is Gaussian noise. The objective of BLDA is to minimize the function:

$$J(\mathbf{w}) = \frac{\beta}{2} \|\mathbf{t} - \mathbf{w}^T \boldsymbol{\phi}(\mathbf{x})\|_2^2 + \frac{\alpha}{2} \mathbf{w}^T \mathbf{w} \quad (6)$$

where α and β are inferred automatically from data by using a Bayesian framework.

2.6 Error-Related Potentials behaviour

Once the ErrPs were identified from Cz and FCz electrodes, xDAWN and FSS algorithms, from both sessions (session 1 and session 2) and C and NC conditions ERP analysis at the average and single trial levels were calculated to characterize and validate the quality of the results obtained. In particular, ERP analysis was performed on Session 1 and Session 2 to evaluate the stability of ERP at different periods of time and between NC and C. All the trials were epoched (-1000 to 1000 ms) and were baseline corrected for the interval from -1000 to 0 ms. We performed pointwise statistical analysis on the averaged waveforms conducting two-sample permutation t-tests (5000 permutations) on every point of the ERP waveform (0-1000 ms). We used False Discovery Rate (FDR) to correct for multiple comparisons.

3. Results

In this section, a qualitative and quantitative comparison among single-channels (FCz and Cz), xDAWN and FSS spatial filter is presented. Afterwards, classification results among single-channels (FCz and Cz), xDAWN and FSS is reported as well.

3.1 Error-Related Potentials on Cz and FCz

Consistently with previous studies [1][21], EEG error-related activity appears in fronto-central areas, as illustrated by the scalp topographical maps in Fig. 1. The figure 1 also shows the grand average ERP for the C and NC conditions for Cz and FCz electrodes in both sessions (sessions 1: thick blue line and session 2: red dashed line). In particular, NC condition refers to the trials that elicited ErrPs (i.e., the cursor moves in the wrong direction) and C condition refers to the trials that do not elicited ErrPs (i.e., the cursor moves in the right direction).

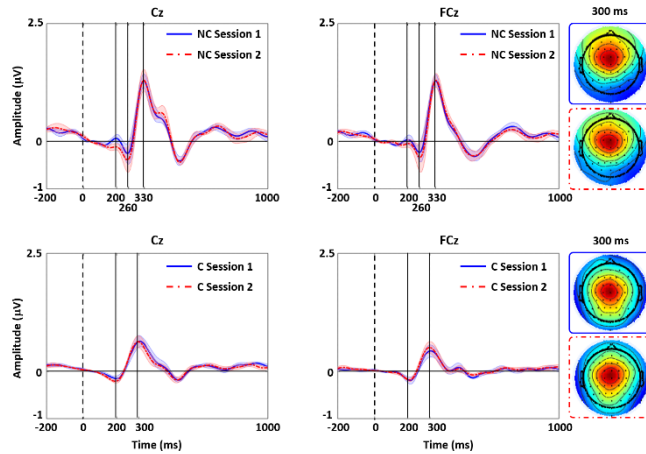


Fig. 1. ERPs and topography map session 1 vs. session 2 - Grand average event related potentials between session 1 (blue thick line) and session 2 (red dashed line) for non-corrected trials (NC: first row) and corrected trials (C: second row). First column shows the ERPs on the Cz electrode for the two recording sessions and second column shows the ERPs on the FCz electrode for the two recording sessions as well. Last column shows scalp topographical maps at 300ms for session 1 (blue square thick line) and session 2 (red square dashed line). Shaded area of the same color highlighting standard error. No sessions differences were observed between NC Session 1 vs. NC Session 2 and C Session 1 vs. C Session 2 (point-by-point permutation t-test at $p < 0.05$).

In all cases, in Fig. 1, the waveforms are characterized by a small positive peak near 200 ms after delivery of feedback for the NC and a negative one for the C, followed by a positive peak around 330 and 300 ms for the NC and C respectively. It should be noted that for the NC a negative deflection around 260 ms is also shown. The stability observed between Session 1 and Session 2 of these signals is a key issue for their use especially for BCI applications. In fact, comparison of the ERPs for the two different recording days (Session 1 and Session 2) shows that the signal remains stable over several weeks (see Fig. 1). In particular, the first three ERP components for the NC (i.e., negative peak at 260 ms and two positive peaks at 200 ms and 330 ms) and the first two peaks for the C (i.e. negative peak at 200 ms and the positive one at 300 ms) are stable between the two recording sessions. No significant difference was found between sessions (point-by-point permutation t-test at $p < 0.05$).

On the other hand, statistically significant differences (point-by-point permutation test $p < 0.05$) between NC and C ERPs were found in both sessions (Fig. 2).

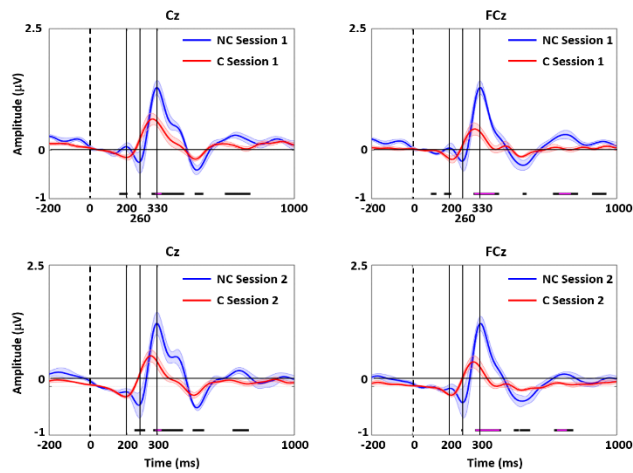


Fig. 2. ERPs non-corrected trials (NC) vs. corrected trials (C) - Grand average event related potentials between non-corrected trials (NC: blue line) and corrected trials (C: red line) for session 1 (first row) and session 2 (second row). First column shows the ERPs on the Cz electrode for NC and C and second column shows the ERPs on the FCz electrode for the NC and C as well. Shaded area of the same colour highlighting standard error. Horizontal black and magenta lines, on the bottom of the figure, indicate a significant group difference between NC vs. C for Session 1 (first row) and Session 2 (second row). Permutation t-test at $p < 0.05$ (black line); $pFDR < 0.05$ (magenta line).

3.2 Event-Related Potentials extracted by xDAWN and FSS

xDAWN and FSS (Fig. 3) as well as Cz and FCz electrodes, show the stability between the two sessions (no significant difference was found, point-by-point permutation t-test at $p < 0.05$). Instead, statistical difference was observed comparing NC vs. C in both xDAWN and FSS algorithms. In particular, we can observe that only the FSS survive for the multiple comparison correction ($pFDR < 0.05$) emphasising that FSS at the average level is more robust in discriminating NC vs. C conditions (Fig. 4).

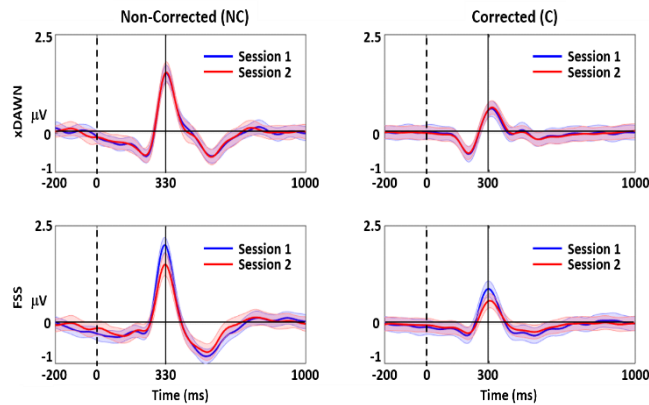


Fig. 3. ERPs session 1 vs. session 2 - Grand average event related potentials between session 1 (blue line) and session 2 (red line) for non-corrected trials (NC: first column) and corrected trials (C: second column). First row shows the ERPs for the xDAWN for the two recording sessions and second row shows the ERPs for the FSS for the two recording sessions as well. Shaded area of the same color highlighting standard error. No sessions differences were observed between NC Session 1 vs. NC Session 2 and C Session 1 vs. C Session 2 (point-by-point permutation t-test at $p < 0.05$).

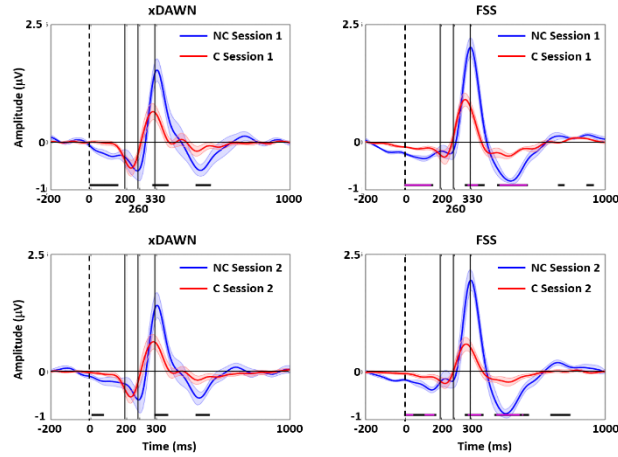


Fig. 4. ERPs non-corrected trials (NC) vs. corrected trials (C) - Grand average event related potentials between non-correct trials (NC: blue line) and corrected trials (C: red line) for session 1 (first row) and session 2 (second row). First column shows the ERPs for the xDAWN for NC and C and second column shows the ERPs for the FSS for the NC and C as well. Shaded area of the same color highlighting standard error. Horizontal black and magenta lines, on the bottom of the figure, indicate a significant group difference between NC vs. C for Session 1 (first row) and Session 2 (second row). Permutation t-test at $p < 0.05$ (black line); pFDR < 0.05 (magenta line).

3.3 Single-Trial Classification

The use of ErrPs in practical BCI applications requires their accurate recognition on a single-trial basis. Following previous studies, we classify the signals using a classifier based on the BLDA, as described in [15][25].

Classification analysis was performed on Cz, FCz electrodes and using advanced source extraction algorithms such as FSS [21][35] and xDAWN. In this work, for xDAWN training we considered $\gamma=0.8$ since with this value we achieved the best classification accuracy in the training dataset. We assess single trial classification of ErrPs using the first dataset to train the spatial filters and the BLDA classifier and the second session as testing set. This allows us to evaluate the feasibility of recognizing such signals using classifiers built on data recorded several weeks before.

Fig. 5 shows the Receiver Operating Characteristic (ROC) curves for classification using the training data (i.e., session 1). The methods FSS, xDAWN and the single channels Cz, FCz are compared. The panels 5(a), 5(b), 5(c), 5(d), 5(e) and 5(f) show the classification results for each subject. The FSS algorithm is able to detect the elicited ErrPs better than the other methods. Fig. 6 shows the ROC curves for classification using the testing data (i.e., session 2). It is clear as the FSS algorithm is able to detect the elicited ErrPs better than the other methods, whereas the xDAWN achieves comparable results to the single channels FCz and Cz.

Table 1 shows in detail the classification accuracy and the Area Under Curve (AUC) for each subject and method using the training data (i.e., session 1). The results, shown in the Table 1, reveals as the FSS outperforms the other methods in terms of classification accuracy both in the case of NC and C. Table 2 shows the classification accuracy for each subject and method using the testing data (i.e., session 2). The results of FSS, shown in Table 2, reveals successful single-trial classification is achieved for both classes with higher detection of C (mean classification accuracy of 95% and 81% for C and NC, respectively).

Best performances are observed for subjects 1, 2, 3, 4 and 5 for whom the recordings were about seven weeks apart for subjects 1, 2 and 3 and 200 days apart for subject 4 and finally 600 days apart for subject 5. In addition, it must be noticed that reasonably good performances are also achieved for subject 6, whose recordings were around 650 days apart. The comparison of the ERPs for the two different recording days shows that classification accuracy remains stable over a long time.

Finally, Table 3 shows the overall performances in terms of accuracy, sensitivity, specificity and F1-score, revealing that the FSS based spatial filter overcomes the other methods of about 20% in all indexes.

It is worth to note that the average classification accuracy reached by the FSS algorithm outperforms the classification results obtained in [1].

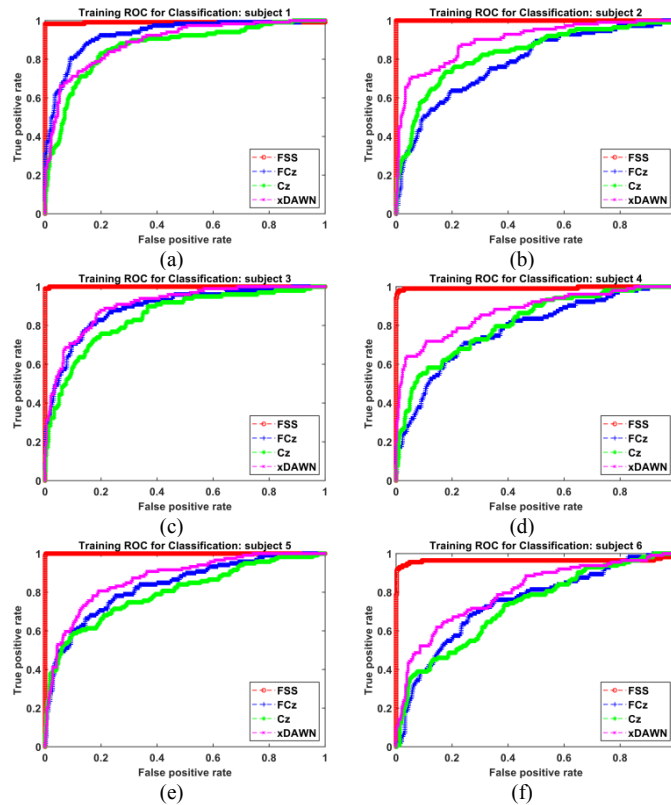


Fig. 5. ROC for classification by BLDA, training data (i.e., session 1) and single channel. The single channels are FCz, Cz and the best channel of FSS and XDAWN. (a) ROC for classification of ErrPs elicited by subject 1, (b) ROC for classification of ErrPs elicited by subject 2, (c) ROC for classification of ErrPs elicited by subject 3, (d) ROC for classification of ErrPs elicited by subject 4, (e) ROC for classification of ErrPs elicited by subject 5, (f) ROC for classification of ErrPs elicited by subject 6.

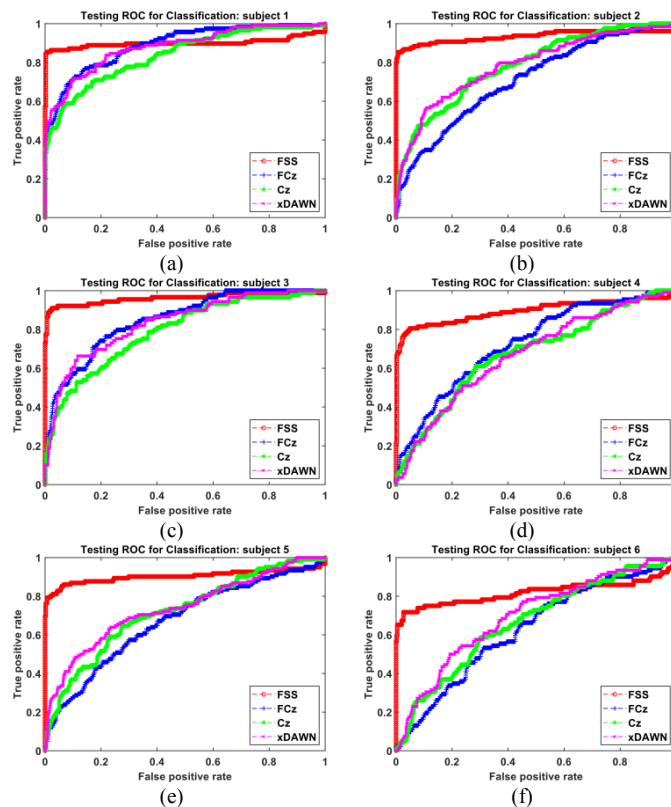


Fig. 6. ROC for classification by BLDA, testing data (i.e., session 2) and single channel. The single channels are FCz, Cz and the best channel of FSS and XDAWN. (a) ROC for classification of ErrPs elicited by subject 1, (b) ROC for classification of ErrPs elicited by subject 2, (c) ROC for classification of ErrPs elicited by subject 3, (d) ROC for classification of ErrPs elicited by subject 4, (e) ROC for classification of ErrPs elicited by subject 5, (f) ROC for classification of ErrPs elicited by subject 6.

Table 1
Classification accuracy and area under curve of training data (session 1)

Subjects	FCz	Cz	xDAWN	FSS
S1 NC	0.88	0.83	0.78	0.98
S1 C	0.85	0.80	0.83	1.00
S1 AUC	0.93	0.86	0.89	0.99
S2 NC	0.64	0.76	0.87	1.00
S2 C	0.80	0.79	0.77	1.00
S2 AUC	0.78	0.83	0.90	1.00
S3 NC	0.81	0.76	0.86	0.99
S3 C	0.84	0.80	0.81	1.00
S3 AUC	0.89	0.85	0.91	1.00
S4 NC	0.71	0.72	0.72	0.98
S4 C	0.76	0.73	0.89	0.99
S4 AUC	0.78	0.81	0.87	0.99
S5 NC	0.78	0.71	0.81	0.99
S5 C	0.75	0.75	0.81	1.00
S5 AUC	0.83	0.80	0.87	1.00
S6 NC	0.68	0.73	0.67	0.96
S6 C	0.74	0.61	0.80	0.95
S6 AUC	0.75	0.73	0.80	0.96
AVG NC	0.75±0.09	0.75±0.04	0.78±0.08	0.98±0.02
AVG C	0.79±0.05	0.75±0.07	0.82±0.04	0.99±0.02

Table 2
Classification accuracy and area under curve of testing data (session 2)

Subjects	FCz	Cz	xDAWN	FSS
S1 NC	0.77	0.65	0.79	0.87
S1 C	0.85	0.86	0.82	0.90
S1 AUC	0.89	0.84	0.88	0.90
S2 NC	0.53	0.61	0.67	0.81
S2 C	0.77	0.78	0.76	1.00
S2 AUC	0.71	0.79	0.79	0.93
S3 NC	0.81	0.69	0.75	0.84
S3 C	0.71	0.72	0.73	0.99
S3 AUC	0.85	0.79	0.84	0.96
S4 NC	0.63	0.61	0.51	0.80
S4 C	0.70	0.71	0.75	0.95
S4 AUC	0.73	0.68	0.67	0.89
S5 NC	0.57	0.61	0.52	0.79
S5 C	0.69	0.73	0.85	0.99
S5 AUC	0.67	0.72	0.74	0.90
S6 NC	0.37	0.61	0.41	0.76
S6 C	0.76	0.63	0.84	0.84
S6 AUC	0.63	0.66	0.70	0.82
AVG NC	0.61±0.16	0.63±0.03	0.61±0.15	0.81±0.04
AVG C	0.75±0.06	0.74±0.08	0.79±0.05	0.95±0.06

Table 3
Overall performances

		Accuracy	Sensitivity	Specificity	F1-score
Training	FCz	0.78	0.79	0.75	0.79
	Cz	0.75	0.75	0.75	0.75
	xDAWN	0.81	0.82	0.78	0.82
	FSS	0.99	0.99	0.98	0.99
Testing	FCz	0.72	0.75	0.61	0.75
	Cz	0.72	0.74	0.63	0.74
	xDAWN	0.75	0.79	0.61	0.79
	FSS	0.92	0.95	0.81	0.95

4. Conclusions

In this work, a semi-supervised algorithm named Functional Source Separation (FSS) that increases signal-to-noise ratio by using a weighted sum of all electrodes rather than relying on a single, or a small sub-set, of EEG channels was presented and compared with single channel (Cz, FCz) approach and using xDAWN spatial filter as well. Although noninvasive electrophysiological techniques, such as EEG, provide the opportunity to directly measure the activity of large-scale neuronal populations, different challenges remain in characterizing this activity. In particular, electrical potentials generated by neuronal activity are not only detected close to neuronal sources but also at distant sites due to electric field propagation. Therefore, each channel positioned across the whole head derives its signal from more than one source [21,35,43,44]. Since the P300 undeniably arises from a widely distributed network [45–48], electing a channel or averaging a group of channels based on the topographic representation might be misleading if one aims to describe a distributed brain network. In this respect, we believe that methods capable of extracting the neural source under investigation (such as FSS and xDAWN) are suitable to avoid selection of channels and to overcome possibly misleading results. On this respect using ErrPs EEG dataset proposed by [1] as a benchmark we tested channels approach (Cz, FCz) and spatial filter approach such as xDAWN vs. FSS. Despite, a similar behavior obtained for the averaged ERP among methods (Cz, FCz, xDAWN and FSS), at the single trial levels the FSS outperforms the other methods. Quantitatively, the same results are obtained using classification approach as summarized in Table 1 where for each of the subjects, the FSS based spatial filter provides a better single-trial classification in the training and testing data.

Conflict of interest statement

All authors have no financial and personal relationships with other people or organizations that could inappropriately bias the work.

Funding

This research did not receive any specific grant from funding agencies in the public, commercial, or not-for-profit sectors.

References

- [1] R. Chavarriaga, J.D.R. Millán, Learning from EEG error-related potentials in noninvasive brain-computer interfaces, *IEEE Trans. Neural Syst. Rehabil. Eng.* 18 (2010) 381–388. doi:10.1109/TNSRE.2010.2053387.
- [2] P.W. Ferrez, J.D.R. Millán, You are wrong! - Automatic detection of interaction errors from brain waves, in: *IJCAI Int. Jt. Conf. Artif. Intell.*, 2005: pp. 1413–1418.
- [3] R. Chavarriaga, A. Sobolewski, J. del R. Millán, Errare machinale est: The use of error-related potentials in brain-machine interfaces, *Front. Neurosci.* (2014). doi:10.3389/fnins.2014.00208.
- [4] B. Dal Seno, M. Matteucci, L. Mainardi, Online detection of P300 and error potentials in a BCI speller, *Comput. Intell. Neurosci.* 2010 (2010). doi:10.1155/2010/307254.
- [5] A.F. Salazar-Gomez, J. Delpreto, S. Gil, F.H. Guenther, D. Rus, Correcting robot mistakes in real time using EEG signals, in: *Proc. - IEEE Int. Conf. Robot. Autom.*, 2017: pp. 6570–6577. doi:10.1109/ICRA.2017.7989777.
- [6] X. Artusi, I.K. Niazi, M.F. Lucas, D. Farina, Performance of a simulated adaptive BCI based on experimental classification of movement-related and error potentials, *IEEE J. Emerg. Sel. Top. Circuits Syst.* 1 (2011) 480–488. doi:10.1109/JETCAS.2011.2177920.
- [7] I. Iturrate, L. Montesano, J. Minguez, Shared-control brain-computer interface for a two dimensional reaching task using EEG error-related potentials, in: *Proc. Annu. Int. Conf. IEEE Eng. Med. Biol. Soc. EMBS*, 2013: pp. 5258–5262. doi:10.1109/EMBC.2013.6610735.
- [8] M. Falkenstein, J. Hohnsbein, J. Hoormann, L. Blanke, Effects of errors in choice reactiontasks on the ERP under focused and divided attention, *Brunia, C.H.M., Gaillard, A.W.K., Kok, A. (Eds.), Psychophysiological Brain Res.* Tilbg. Univesity Press. Tilbg. (1990) 192 – 195.
- [9] G. Hajcak, N. McDonald, R.F. Simons, To err is autonomic: Error-related brain potentials, ANS activity, and post-error compensatory behavior, in: *Psychophysiology*, 2003. doi:10.1111/1469-8986.00107.
- [10] M. Spüler, C. Niethammer, Error-related potentials during continuous feedback: using EEG to detect errors of different type and severity, *Front. Hum. Neurosci.* 9 (2015) 1–10. doi:10.3389/fnhum.2015.00155.
- [11] P.W. Ferrez, J. Del R. Millán, Error-related EEG potentials generated during simulated brain-computer interaction, *IEEE Trans. Biomed. Eng.* 55 (2008) 923–929. doi:10.1109/TBME.2007.908083.
- [12] R. Chavarriaga, Z. Khaliliardali, L. Gheorghe, I. Iturrate, J.D.R. Millán, EEG-based decoding of error-related brain activity in a real-world driving task, *J. Neural Eng.* 12 (2015). doi:10.1088/1741-2560/12/6/066028.
- [13] S.K. Ehrlich, G. Cheng, Human-agent co-adaptation using error-related potentials, *J. Neural Eng.* 15 (2018). doi:10.1088/1741-2552/aae069.
- [14] C. Lopes Dias, A.I. Sburlea, G.R. Müller-Putz, Masked and unmasked error-related potentials during continuous control and feedback, *J. Neural Eng.* 15 (2018). doi:10.1088/1741-2552/aab806.
- [15] B. Rivet, A. Souloumiac, V. Attina, G. Gibert, xDAWN Algorithm to Enhance Evoked Potentials: Application to Brain-Computer Interface, *IEEE Trans. Biomed. Eng.* 56 (2009) 2035–2043. doi:10.1109/TBME.2009.2012869.
- [16] O. Falzon, K.P. Camilleri, J. Muscat, The analytic common spatial patterns method for EEG-based BCI data, *J. Neural Eng.*

- 9 (2012). doi:10.1088/1741-2560/9/4/045009.
- [17] K. Yu, K. Shen, S. Shao, W.C. Ng, X. Li, Bilinear common spatial pattern for single-trial ERP-based rapid serial visual presentation triage, *J. Neural Eng.* 9 (2012). doi:10.1088/1741-2560/9/4/046013.
- [18] C. Sannelli, C. Vidaurre, K.-R. Müller, B. Blankertz, CSP patches: An ensemble of optimized spatial filters. An evaluation study, *J. Neural Eng.* 8 (2011). doi:10.1088/1741-2560/8/2/025012.
- [19] C. Sannelli, C. Vidaurre, K.-R. Müller, B. Blankertz, Ensembles of adaptive spatial filters increase BCI performance: An online evaluation, *J. Neural Eng.* 13 (2016). doi:10.1088/1741-2560/13/4/046003.
- [20] R. Guarnieri, M. Marino, F. Barban, M. Ganzetti, D. Mantini, Online EEG artifact removal for BCI applications by adaptive spatial filtering, *J. Neural Eng.* 15 (2018). doi:10.1088/1741-2552/aacdf.
- [21] C. Porcaro, J. Henk, D. Mantini, I.H. Robertson, N. Wenderoth, NeuroImage P3b amplitude as a signature of cognitive decline in the older population : An EEG study enhanced by Functional Source Separation, *Neuroimage.* 184 (2019) 535–546. doi:10.1016/j.neuroimage.2018.09.057.
- [22] S. Migliore, G. Curcio, C. Porcaro, C. Cottone, I. Simonelli, G. D’aurizio, D. Landi, M.G. Palmieri, A. Ghazaryan, F. Squitieri, M.M. Filippi, F. Vernieri, Emotional processing in RRMS patients: Dissociation between behavioural and neurophysiological response, *Mult. Scler. Relat. Disord.* 27 (2019). doi:10.1016/j.msard.2018.11.019.
- [23] D. Gutiérrez, D.I. Escalona-Vargas, EEG data classification through signal spatial redistribution and optimized linear discriminants, *Comput. Methods Programs Biomed.* (2010). doi:10.1016/j.cmpb.2009.05.005.
- [24] M. Mohseni, V. Shalchyan, M. Jochumsen, I.K. Niazi, Upper Limb Complex Movements Decoding From Pre-Movement EEG Signals Using Wavelet Common Spatial Patterns, *Comput. Methods Programs Biomed.* (2019). doi:10.1016/j.cmpb.2019.105076.
- [25] B. Rivet, H. Cecotti, A. Souloumiac, E. Maby, J. Mattout, Theoretical analysis of XDAWN algorithm: Application to an efficient sensor selection in a P300 BCI, in: *Eur. Signal Process. Conf.*, 2011: pp. 1382–1386.
- [26] G. Barbati, C. Porcaro, F. Zappasodi, P.M. Rossini, F. Tecchio, Optimization of an independent component analysis approach for artifact identification and removal in magnetoencephalographic signals, *Clin. Neurophysiol.* 115 (2004) 1220–1232. doi:10.1016/j.clinph.2003.12.015.
- [27] C. Porcaro, M.T. Medaglia, A. Krott, Removing speech artifacts from electroencephalographic recordings during overt picture naming, *Neuroimage.* 105 (2015) 171–180. doi:10.1016/j.neuroimage.2014.10.049.
- [28] G. Barbati, C. Porcaro, A. Hadjipapas, P. Adjamian, V. Pizzella, G.L. Romani, S. Seri, F. Tecchio, G.R. Barnes, Functional source separation applied to induced visual gamma activity, *Hum. Brain Mapp.* 29 (2008) 131–141. doi:10.1002/hbm.20375.
- [29] G. Barbati, R. Sigismondi, F. Zappasodi, C. Porcaro, S. Graziadio, G. Valente, M. Balsi, P.M. Rossini, F. Tecchio, Functional source separation from magnetoencephalographic signals, *Hum. Brain Mapp.* 27 (2006) 925–934. doi:10.1002/hbm.20232.
- [30] C. Porcaro, G. Coppola, G. Di Lorenzo, F. Zappasodi, A. Siracusano, F. Pierelli, P.M. Rossini, F. Tecchio, S. Seri, Hand somatosensory subcortical and cortical sources assessed by functional source separation: An EEG study, *Hum. Brain Mapp.* 30 (2009) 660–674. doi:10.1002/hbm.20533.
- [31] C. Porcaro, G. Barbati, F. Zappasodi, P.M. Rossini, F. Tecchio, Hand sensory-motor cortical network assessed by functional source separation, *Hum. Brain Mapp.* 29 (2008) 70–81. doi:10.1002/hbm.20367.
- [32] C. Porcaro, D. Ostwald, A.P. Bagshaw, Functional source separation improves the quality of single trial visual evoked potentials recorded during concurrent EEG-fMRI, *Neuroimage.* 50 (2010) 112–123. doi:10.1016/j.neuroimage.2009.12.002.
- [33] C. Porcaro, D. Ostwald, A. Hadjipapas, G.R. Barnes, A.P. Bagshaw, The relationship between the visual evoked potential and the gamma band investigated by blind and semi-blind methods, *Neuroimage.* 56 (2011) 1059–1071. doi:10.1016/j.neuroimage.2011.03.008.
- [34] F. Tecchio, C. Porcaro, G. Barbati, F. Zappasodi, Functional source separation and hand cortical representation for a brain-computer interface feature extraction, *J. Physiol.* 580 (2007) 703–721. doi:10.1113/jphysiol.2007.129163.
- [35] C. Porcaro, F. Tecchio, Semi-blind Functional Source Separation Algorithm from Non-invasive Electrophysiology to Neuroimaging, in: G.R. Naik, W. Wang (Eds.), *Blind Source Sep. Adv. Theory, Algorithms Appl.*, Springer Berlin Heidelberg, 2014: pp. 521–551. doi:10.1007/978-3-642-55016-4_19.
- [36] O.I. Khan, F. Farooq, F. Akram, M.T. Choi, S.M. Han, T.S. Kim, Robust extraction of P300 using constrained ICA for BCI applications, *Med. Biol. Eng. Comput.* 50 (2012) 231–241. doi:10.1007/s11517-012-0861-4.
- [37] W. Lu, J.C. Rajapakse, Approach and applications of constrained ICA, *IEEE Trans. Neural Networks.* 16 (2005) 203–212. doi:10.1109/TNN.2004.836795.
- [38] S. Wang, C.J. James, Extracting rhythmic brain activity for brain-computer interfacing through constrained independent component analysis, *Comput. Intell. Neurosci.* 2007 (2007). doi:10.1155/2007/41468.
- [39] S. Kirkpatrick, C.D. Gelatt, M.P. Vecchi, Optimization by simulated annealing, *Science* (80-.). 220 (1983) 671–680. doi:10.1126/science.220.4598.671.
- [40] Y. Guo, T. Hastie, R. Tibshirani, Regularized linear discriminant analysis and its application in microarrays, *Biostatistics.* 8 (2007) 86–100. doi:10.1093/biostatistics/kxj035.
- [41] U. Hoffmann, J.M. Vesin, T. Ebrahimi, K. Diserens, An efficient P300-based brain-computer interface for disabled subjects, *J. Neurosci. Methods.* 167 (2008) 115–125. doi:10.1016/j.jneumeth.2007.03.005.
- [42] D.J.C. Mackay, N. Systems, Bayesian Interpolation, *Neural Comput.* 4 (1992) 415–447. doi:10.1162/neco.1992.4.3.415.
- [43] M. Rusiniak, M. Lewandowska, T. Wolak, A. Pluta, R. Milner, M. Ganc, A. Włodarczyk, A. Senderski, L. Śliwa, H. Skarżyński, A modified oddball paradigm for investigation of neural correlates of attention: A simultaneous ERP-fMRI study, *Magn. Reson. Mater. Physics, Biol. Med.* 26 (2013) 511–526. doi:10.1007/s10334-013-0374-7.
- [44] M. Siegel, T.H. Donner, A.K. Engel, Spectral fingerprints of large-scale neuronal interactions, *Nat. Rev. Neurosci.* (2012). doi:10.1038/nrn3137.
- [45] A.M. Fjell, K.B. Walhovd, B. Fischl, I. Reinvang, Cognitive function, P3a/P3b brain potentials, and cortical thickness in aging, *Hum. Brain Mapp.* 28 (2007) 1098–1116. doi:10.1002/hbm.20335.
- [46] D.E.J. Linden, The P300: Where in the Brain Is It Produced and What Does It Tell Us?, *Neurosci.* 11 (2005) 563–576.

doi:10.1177/1073858405280524.

- [47] F. Barcelo, Detection of change: event-related potential and fMRI findings, *Clin. Neurophysiol.* 115 (2004) 1712–1713.
doi:10.1016/j.clinph.2004.02.002.
- [48] J. Polich, Updating P300: An integrative theory of P3a and P3b, *Clin. Neurophysiol.* 118 (2007) 2128–2148.
doi:10.1016/j.clinph.2007.04.019.

Conflict of interest statement

All authors have no financial and personal relationships with other people or organizations that could inappropriately bias the work.